HHS Public Access

Author manuscript

J Bone Miner Res. Author manuscript; available in PMC 2016 November 14.

Published in final edited form as:

J Bone Miner Res. 2014 November ; 29(11): 2346–2356. doi:10.1002/jbmr.2274.

Botulinum Toxin Induces Muscle Paralysis and Inhibits Bone Regeneration in Zebrafish

Anthony M. Recidoro[1,4], **Amanda C. Roof**[1,4], **Michael Schmitt**[1], **Leah E. Worton**[1], **Timothy Petrie**[2], **Nicholas Strand**[2], **Brandon J. Ausk**[1], **Sundar Srinivasan**[1], **Randall T. Moon**[2], **Edith M. Gardiner**[1], **Werner Kaminsky**[3], **Steven D. Bain**[1], **Christopher H. Allan**[1], **Ted S. Gross**[1], and **Ronald Y. Kwon**[1,5]

[1]Department of Orthopaedics and Sports Medicine, University of Washington, Seattle, Washington, USA

[2]Howard Hughes Medical Institute, Department of Pharmacology, Institute for Stem Cell and Regenerative Medicine, University of Washington, Seattle, Washington, USA

[3]Department of Chemistry, University of Washington, Seattle, Washington, USA

Abstract

Intramuscular administration of Botulinum toxin (BTx) has been associated with impaired osteogenesis in diverse conditions of bone formation (e.g., development, growth, and healing), yet the mechanisms of neuromuscular-bone crosstalk underlying these deficits have yet to be identified. Motivated by the emerging utility of zebrafish (*Danio rerio*) as a rapid, genetically tractable, and optically transparent model for human pathologies (as well as the potential to interrogate neuromuscular-mediated bone disorders in a simple model that bridges *in vitro* and more complex *in vivo* model systems), in this study we developed a model of BTx-induced muscle paralysis in adult zebrafish, and examined its effects on intramembranous ossification during tail fin regeneration. BTx administration induced rapid muscle paralysis in adult zebrafish in a manner that was dose-dependent, transient, and focal, mirroring the paralytic phenotype observed in animal and human studies. During fin regeneration, BTx impaired continued bone ray outgrowth, morphology, and patterning, indicating defects in early osteogenesis. Further, BTx significantly decreased mineralizing activity and crystalline mineral accumulation, suggesting delayed late-stage osteoblast differentiation and/or altered secondary bone apposition. Bone ray transection proximal to the amputation site focally inhibited bone outgrowth in the affected ray, implicating intra- and/or inter-ray nerves in this process. Taken together, these studies demonstrate the potential to interrogate pathological features of BTx-induced osteoanabolic dysfunction in the regenerating zebrafish fin, define the technological toolbox for detecting bone growth and mineralization deficits in this process, and suggest that pathways mediating neuromuscular regulation of osteogenesis may be conserved beyond established mammalian models of bone anabolic disorders.

[5]Corresponding author: ronkwon@uw.edu.
[4]These authors contributed equally to this work

Keywords

Animal Models; Bone Modeling and Remodeling; Osteoblasts; Skeletal Muscle; Bone-Brain-Nervous System Interactions

INTRODUCTION

The growing use of simple model organisms for examining human disease, in conjunction with modern advances in large-scale biological research (e.g., rapid whole-genome sequencing, high-throughput chemical discovery, and high-content imaging), underscore the potential impact of novel vertebrate models of bone pathologies that are genetically tractable, optically transparent, and amenable to large-scale experimental paradigms. Within the last several decades, zebrafish (*Danio rerio*) have emerged from their longstanding use as a vertebrate model of developmental biology to a valuable model organism for human disease. This emergence has been spurred by their unique experimental attributes (e.g., optical transparency, ease of genetic manipulation, small size, low cost, and the ability to rapidly administer compounds via the water) that enable powerful experimental approaches that would otherwise be highly challenging in other vertebrate model systems (e.g., large-scale genetic screens, high-content imaging of cellular dynamics, *in vivo* small molecule discovery, and rapid interrogation of human mutant gene function) (1).

Though the zebrafish skeleton differs from that in mammals in several aspects (such as a lack of hematopoietic tissue-containing bone marrow, diminished participation in calcium homeostasis, and a reduced role in resisting gravitational loading (2)), it is becoming increasingly clear that it also retains a number of conserved elements with significant potential to recapitulate human bone native and disease states. For example, zebrafish possess the major cellular constituents of mammalian bone (osteocytes, osteoblasts, and osteoclasts) and have a high degree of homology for genes mediating mammalian osteogenesis and bone homeostasis (both in regard to amino acid sequence and expression patterns) (3). In addition, zebrafish respond to several known osteoactive compounds in humans (4,5), and express a number of orthologous genes implicated in mammalian skeletal disease (including those identified in human genome-wide association studies (6)). These attributes have spurred significant interest in examining the potential of zebrafish to recapitulate mammalian bone pathophysiologies under developmental, homeostatic, and/or regenerative conditions (3,7,8).

Neuromuscular-mediated bone disorders (i.e., bone pathologies associated with abnormal neuronal and/or muscular function such as disuse, neurological trauma, and paralysis) are mediated by complex mechano-chemical interactions between diverse cell types (neuronal, muscle, bone, endothelial, etc.). Given the experimental challenges in recapitulating these interactions *in vitro*, zebrafish may hold unique potential to bridge existing cell culture and animal models (9–12) by enabling their *in vivo* interrogation in a rapid, genetically tractable, and optically transparent model system. An essential first step toward such examinations is characterizing the potential for the zebrafish skeleton to recapitulate known associations between inhibitors of neuromuscular activity and impaired skeletal function. For example,

intramuscular injection of Botulinum toxin (a clostridial neurotoxin that inhibits synaptic fusion) has been broadly shown to induce rapid muscle paralysis and diminished skeletal function in a variety of conditions and model organisms. In skeletally mature mice, intramuscular injection in the hindlimb induces rapid endosteal bone resorption but minimally alters periosteal bone formation (11). Interestingly, recent studies suggest this loss is not entirely attributable to deficits in mechanical loading (13), and may be mediated in part through disruption of proprioceptive nerve function (14). In contrast, under conditions of skeletogenesis, BTx is associated with altered patterning and diminished bone mass in broad contexts including bone and joint development (15), fracture callus formation (16), appositional growth (17), cortical defect healing (18), and mandibular development (19). The diversity of contexts in which BTx-induced bone anabolic dysfunction is manifested suggests that this physiology may be conserved in broad conditions of osteogenesis, and consequently, the potential to interrogate it in novel *in vivo* models apart from those established for mammalian bone pathologies.

By virtue of its capacity to recapitulate bone anabolic pathways associated with mammalian osteogenesis, osteoblast differentiation, and limb development (20,21), the regenerating zebrafish tail fin represents a potentially powerful model system for such studies. Like other teleosts, zebrafish possess the capacity to regenerate amputated fin bone rays via epimorphic regeneration. Following fin amputation, osteoblasts at the stump partially de-differentiate to form part of the proliferating blastema (22), which gives rise to differentiating (or re-differentiating) osteoblasts that undergo bone matrix secretion and mineralization (22,23). The rate of bone formation during this process is remarkable, as new bone segments are readily observed within 3–5 days following amputation (with the majority of lost bone, joints, nerves, skin and blood vessels restored within a few weeks). Experimentally, the regenerating fin confers a number of favorable attributes including a simple anatomical structure (segmented bony rays encapsulating intra-ray nerves, vasculature, and connective tissue), the capacity to rapidly manipulate gene expression (24), amenability to chemical and genetic screening (25,26), and the potential to image cell dynamics *in vivo*. In addition, the tail fin possesses skeletal muscle only at its base, enabling the opportunity to examine remote effects of BTx-induced neuronal dysfunction in a manner that minimizes the influence of impaired muscle on bone outgrowth at the distal tip.

In this study, we developed a model of BTx-induced muscle paralysis in adult zebrafish, and examined its effects on intramembranous ossification during tail fin regeneration. Our investigations demonstrate the potential for BTx to induce focal and transient paralysis in zebrafish, show the capacity for this impairment to induce altered bone ray outgrowth, patterning, and mineralization, and highlight a potential role for inter- and/or intra-ray nerves in regulating this process. Collectively, our studies demonstrate the potential to interrogate pathological features of BTx-induced osteoanabolic dysfunction in the regenerating zebrafish tail fin, define the technological toolbox for detecting bone growth and mineralization deficits in this process, and suggest that pathways mediating neuromuscular regulation of osteogenesis may be conserved beyond established mammalian models of bone anabolic disorders.

MATERIALS AND METHODS

Zebrafish

Adult wild-type zebrafish (outbred stock) were purchased from Aquatic Research Organisms and housed at a temperature of 27–28°C on a 14:10h light:dark photoperiod. All studies were performed in mixed sex adult zebrafish (~30mm S.L.).

Botulinum Toxin Administration

Botulinum Toxin A (Botox, Allergan) and Botulinum Toxin B (Myobloc, Solstice Neurosciences) were prepared/diluted in saline. Fish were anesthetized in 0.04% MS-222 (Sigma), injected using a Nanofil microinjection system (10μL syringe, 33–35 gauge needle), and recovered in fresh water. An injection volume of 5μL was used for all experiments.

Tail Fin Amputations

For tail fin amputations, zebrafish were anesthetized, injected with BTx or saline, and immediately subjected to ~50% amputation using a straight razor blade. Following amputation, fish were recovered in fresh water. Brightfield images of the caudal fin were acquired on a stereomicroscope. Images were analyzed for the following quantities: fin area, length of the longest fin rays in the dorsal and ventral lobes, and length of the shortest fin ray in the middle of the fin. Percent regrowth was computed as described in (27).

Bone Ray Transection

For bone ray transections, fish were anesthetized, and a 0.5mm hole was resected from a single bone ray approximately 0.5–1.0mm proximal to the amputation plane using a tissue micro-punch (Harris Uni-core). The position and size of the defect were selected based on the average inter-ray distance of ~0.25mm between the transected ray and its dorsal/ventral neighbors, as well as our desire to transect the majority of intra- and inter-ray nerves associated with the affected ray. All transections were performed on the fourth most dorsal ray, with the fourth most ventral ray serving as an internal control.

Locomotor Scoring

For locomotor function assessment, zebrafish were scored on a scale of 1–5 using criteria adapted from Goldshmit et al. (28): 1: complete paralysis, with fish resting on the bottom of the tank; 2: infrequent jerky movements but no directed motion; 3: some directed motion through a series of small jerky movements; 4: large muscle movements with coordinated, whole-body rotations while turning; 5: indistinguishable from uninjected fish.

Open Field Activity Monitoring

For open field activity assessment, fish were placed in an activity monitor (Med Associates) in 20×8×10cm tanks filled with 250mL system water. Fish motions were tracked over a 20min period using Med Associates software. Distance, time spent swimming, and swimming velocity were computed from swim traces. Videos of fish swimming were

observed and evaluated for leftward (counter clockwise) and rightward (clockwise) turns while swimming.

Startle Response Testing

For startle response testing, fish were placed in 10cm diameter cylindrical tanks filled with 150mL of system water. Audible startles were invoked by dropping an aluminum weight mounted to a lever arm (to ensure consistent drop heights). Video recordings of the C-start response (250fps) were captured using a high-speed video camera (Kodak Ektapro).

Real-time RT-PCR

For real-time RT-PCR, regenerated fin tissue was isolated from anesthetized fish and immediately immersed in RNAlater storage solution (Qiagen). Total RNA was extracted using the RNeasy Mini Kit (Qiagen) according to manufacturer's protocol. cDNA was synthesized using Super Script III reverse transcriptase (Invitrogen), and real-time PCR was performed using SYBR green and the Applied Biosystems Viia7 Real time PCR system. Relative gene expression levels were quantified using the 2^(−ΔΔCT) method with beta-actin as the housekeeping gene. The following sequences were used: gli1 F: 5′-CAGCTCCGCAAGTTTTCCAG-3′, gli1 R: 5′-TGGTTGCTGGTGTTGTCGTA-3′; ptch1 F: 5′-GGAATGCGACTGGGAGGAAA-3′, ptch1 R: 5′-CCTGACGAGGCGTCTGTATC-3′; shha F: 5′-ACTGTCTCGCCTAGCTGTGG-3′, shha R: 5′-CCTTCTGTCCTCCGTCCTG-3′; shhb F: 5′-CCACGATCCGACAACGAGAA-3′, shhb R: 5′-AGGCTCTCGCATGTGTCTTC-3′; smo F: 5′-CACGCACACGTCTCTGATTC-3′, smo R: 5′-TCCACCTTTCCATTCTCACAC-3′; msxb F: 5′-GACGACAGTGAAGAACTAAGCG-3′, msxb R: 5′-CCGTTCGGCGATAGAGAGGT-3′; pcna F: 5′-CCCGATTGTGACCCTCTAAA-3′, pcna R: 5′-TTGGAATGAGCAGTTGGACA-3′; beta-actin F: 5′-CAACAGGGAAAAGATGACACAGAT-3′, beta-actin R: 5′-CAGCCTGGATGGCAACGT-3′.

Quantitative Fluorochrome Analysis

Live fish were immersed in buffered 0.04% calcein and rinsed for 10min in fresh water (29). For each fin, a composite image stack (4×9×10 images in the x/y/z directions) was acquired on a high-content fluorescent microscopy system (Zeiss Axio Imager.M2, constant settings for all experiments), and the maximum intensity projection (MIP) computed (~5000×9000 pixels, 1.3μm/pixel). Calcein intensities were evaluated at the midpoints of the regenerated bone segments, and these data were used to compute mean calcein intensity (μ), standard deviation (σ), and coefficient of variation (σ/μ) for each fish. Alizarin red staining was performed using identical procedures.

Rotopol Microscopy

A Rotopol microscopy system was used to compute bone ray birefringence in hydrated fixed fins. Our use of this modality enabled the independent computation of birefringence, transmittance, and orientation, quantities that are typically coupled in polarized light imaging (30). Briefly, a custom polarizing microscope was adapted with a stepper motor,

rotating-polarizer, and circular analyzer (consisting of a linear analyzer and quarter waveplate aligned at 45°). A digital camera was used to acquire a sequence of images under a step-wise rotating polarizer. Using the relations in (30), birefringence (|sinδ|), transmittance, and orientation were computed on a pixel-by-pixel basis. For analysis, composite images of birefringence (9 fields of view manually stitched together) were generated for each fin, non-regenerated (i.e., proximal to the amputation plane) and regenerated tissue (i.e., distal to the amputation plane) were manually segmented, and mean values of |sinδ| within each tissue region were computed.

Data Analysis and Statistics

Comparison between two groups was performed using a t-test assuming equal variances and a two-tailed distribution. Differences in distributions were assessed using a two-sample Kolmogorov-Smirnov test (31). For multiple comparisons, either one-way ANOVA and Fisher's PLSD post-hoc tests or two-way ANOVA was performed. $p<0.05$ was considered statistically significant. All data are presented as mean±SE.

RESULTS

Intramuscular administration of BTxB, but not BTxA, induces dose- and site-specific deficits in locomotor function

We first assessed the capacity for two mechanistically distinct Botulinum toxin serotypes to induce muscle paralysis in adult zebrafish: Botulinum Toxin A (BTxA) and Botulinum toxin (BTxB). BTxA inhibits synaptic fusion by cleaving the t-SNARE SNAP-25, while BTxB inhibits the v-SNARE synaptobrevin. BTx was injected intramuscularly into one of two locations: 1) the dorsolateral trunk, or 2) at the base of the tail fin (Fig 1A), and locomotor function was evaluated 3 days post injection (a time point in which BTx-induced deficits appeared to largely plateau). Locomotor scoring revealed fish injected in the trunk with 0.5U BTxB, but not 0.5U BTxA, exhibited a significant reduction ($p<0.001$) in locomotor function relative to trunk-injected fish administered saline (Fig 1B). In addition, fish administered 0.5U BTxB in the trunk exhibited significantly greater deficits than those administered an equivalent BTxB dose at the base of the tail ($p<0.05$), suggesting that the severity of BTxB-induced deficits was site-specific and graded along the anteroposterior axis. In tail-injected fish, animals injected with 0.1U BTxB ($p<0.05$) but not 0.05U BTxB exhibited significant decreases in locomotor function compared to tail-injected fish administered saline, suggesting the potential for BTxB to induce graded paralysis in zebrafish by modulating injection dosage.

BTxB-injected fish exhibit transient deficits in open-field swimming activity

Given the potential for disuse to contribute to aberrant bone regeneration, we next investigated whether BTxB-induced locomotor deficits were translated into reduced open field swimming activity (and if so, the degree to which these deficits were transient). At 7dpi (days post injection), tail-injected fish administered 0.1U BTxB exhibited a significant decrease in swimming distance compared to saline controls ($p<0.01$) that was attributable to both a significant reduction in time spent swimming ($p<0.001$) as well as a decrease in swimming velocity ($p<0.001$) (Fig 2A). At 14dpi, BTxB-injected fish also exhibited a

significant decrease in swim distance ($p<0.05$), swim velocity ($p<0.05$), and time spent swimming ($p<0.01$). However, no significant differences in these quantities were observed at 49dpi. These studies suggest the potential for BTxB to induce transient deficits in open field activity that are sustained through a period of time sufficient for substantial fin regeneration to occur (14 days), but recoverable in the long-term.

Asymmetric swimming tendencies in BTxB-injected fish indicate focal muscle paralysis

We next examined the degree to which BTxB-induced paralysis was focal to the site of injection. For these studies, our strategy was to inject fish on the right dorsolateral surface of the trunk, and monitor for asymmetric swimming behaviors arising from unilateral impairment of muscle contractility. During open field swimming, fish administered 0.5U BTxB exhibited a significantly lower tendency to turn in the rightward (clockwise) direction ($p<0.05$) compared to uninjected controls and fish injected with BTxA (Fig 2B), consistent with disproportionate left/right muscle impairment. To determine whether deficits were focal along the anteroposterior axis, we performed startle response testing to invoke the startle-induced C-start response (32). BTxB-injected fish exhibited a W-shaped body plan during rightward, but not leftward C-starts, with the mid-apex corresponding to the site of injection (Fig 2C). This was in contrast to uninjected fish and trunk-injected fish administered saline, which exhibited highly pronounced full-length body flexions in both the leftward and rightward directions. Collectively, these studies suggest the potential for intramuscular injection of BTxB to induce focal impairment of contractile function in both the mediolateral and anteroposterior axes.

BTxB-injected fish exhibit decreased area of fin regrowth during late, but not early, stages of regenerative outgrowth

Next, we investigated whether BTxB-induced impairment of the tail fin neuromuscular tissue was associated with bone regenerative dysfunction. Fin regeneration occurs through three sequential stages: wound healing (0–1 days post amputation (dpa)), blastema formation (1–2dpa), and regenerative outgrowth (>2dpa) (33). In this case, we assessed bone ray regrowth at 5dpa, 9dpa, and 12dpa, resulting in ~3–4 days of regenerative outgrowth within three different periods of time (2–5dpa, 5–9dpa, 9–12dpa). By 9dpa, tail-injected fish administered 0.1U BTxB exhibited noticeable deficits in length of bone ray regrowth (Fig 3A). Quantitative image analysis at the same time point revealed that the BTxB-induced reduction in the percent length of bone ray regrowth was more pronounced in the middle fin rays relative to dorsal and ventral rays ($p<0.05$ for BTxB:ray interaction, $p<0.001$ for BTxB) (Fig 3B). Quantification of percent area of fin regrowth revealed a significant decrease in BTxB-injected fish at 9dpa ($p<0.001$) and 12dpa ($p<0.01$). However, no difference in regrowth was observed at 5dpa (Fig 3C), suggesting BTxB impaired continued bone ray outgrowth, but not its initialization.

Intramuscular BTxB injection alters bone ray segment morphology, branching, and joint specification

Previous studies in the regenerating fin have demonstrated an association between a lack of sustained bone outgrowth and impaired spatial specification of osteoblast differentiation (34). In this case, we examined the potential for BTxB to alter the latter as evidenced by

altered bone segment morphology, ray branching, and joint specification. Quantitative image analysis at 9dpa revealed that BTxB-injected fish exhibited a significant reduction in the average number of segments in the regenerated ray ($p<0.01$, Fig 4A) bone segment width ($p<0.01$, Fig 4C), inter-joint distance (i.e., bone segment length, $p<0.05$, Fig 4B), and bone ray branching ($p<0.01$, Fig 4D). Notably, the latter two quantities (inter-joint distance and bone ray branching) are direct measures of bone patterning as they cannot be manifested through deficits in osteoblast activity alone. Thus, these results suggest that BTxB impaired bone ray morphogenesis, and implicate spatial specification of osteoblast differentiation (i.e., patterning) in this process.

BTxB-injected fish exhibit impaired mineralizing activity in newly regenerated bone segments

We further investigated the potential for BTxB to impair mineralization during late-stage osteoblast differentiation. We first performed *in vivo* calcein labeling (29) to examine actively mineralizing surfaces in newly regenerated bone segments. Qualitatively, saline-injected fish exhibited uniform and high-intensity calcein labeling in the regenerated tissue, in contrast to the low-intensity labeling in proximal non-regenerated bone (Fig 5A–A′). Unlike saline-injected fish, fish treated with BTxB generally exhibited heterogeneous, “patchy” labeling in the regenerate with a high degree of phenotypic variation from fish-to-fish. In particular, BTxB-treated fish exhibited varying mixtures of inter-ray heterogeneity (i.e., marked differences in labeling between rays, Fig 5B) and intra-ray heterogeneity (i.e., sporadic regions of low and high labeling along individual rays, Fig 5B′). To quantify these deficits, we evaluated calcein intensities in over 900 individual bone segments and generated probability distribution functions for saline- and BTxB-injected fish (Fig 5C). Distributional analysis revealed highly significant differences in the intensity distributions of these two populations ($p<0.001$). More specifically, BTxB-treated fish exhibited a higher proportion of low intensity segments, a lower proportion of segments with medium intensity segments, and a roughly equal probability of high intensity segments. Quantification of the coefficient of variation of intensity ($p=0.05$, Fig 5D), a normalized measure of relative dispersion, suggested BTxB induced greater heterogeneity of labeling within each fish (consistent with our qualitative observations). No significant difference in the mean intensity of labeling between saline- and BTxB-injected fish was detected ($p=0.48$, Fig 5E), potentially attributable to the higher inter-specimen variability in BTxB-treated animals.

Rotopol microscopy reveals BTxB-injected fish exhibit impaired crystalline mineral accumulation

To determine whether BTxB-injected fish exhibited a functional deficit in mineralization, we subjected zebrafish to quantitative polarized light imaging using Rotopol microscopy (30) (Fig 6A). Previous studies suggest that zebrafish fin ray birefringence is primarily associated with crystalline mineral accumulation rather than matrix anisotropy (except for between segments, where there is additional birefringence due to the fibrous inter-segment ligament) (35). BTxB-injected fish exhibited significantly decreased birefringence in the regenerated (but not non-regenerated) tissue ($p<0.05$, Fig 6B). These results indicate that BTx impaired crystalline mineral accumulation during bone regeneration, suggesting delayed late-stage differentiation during initial ossification and/or decreased secondary bone apposition.

Proximal bone ray transection impairs outgrowth in a focal manner

The remote effects of BTx-induced neuromuscular impairment on regenerative outgrowth and bone cell differentiation at the distal tip of the fin suggested a potential role for intra- and inter-ray nerves in mediating these long-distance effects (for example, through direct nerve-bone cell crosstalk, or indirectly via epithelial or endothelial intermediaries). To explore this possibility, we generated circular lesions proximal to the amputation stump to focally transect intra-ray nerves, blood vessels, and associated inter-ray nerves within a single bone ray. Fish subjected to bone ray transection exhibited impaired regenerative outgrowth in a manner that was highly focused to the affected ray (Fig 7A). In particular, we observed a significant reduction in the length of the regenerate in transected rays compared to immediately neighboring dorsal/ventral rays (67.5±9.3% at 7dpa, $p=0.03$, $n=5$), with no such reduction observed in untransected control rays (104.0±3.7%, $p=0.34$, $n=5$). Calcein labeling was also reduced within the regenerate in 67% (6/9) of the transected rays (Fig 7B).

BTxB alters sonic hedgehog pathway gene expression

Finally, to explore the pathways linking BTxB-induced neuromuscular impairment to bone regenerative deficits, we analyzed gene expression for components of the sonic hedgehog pathway (shha, shhb, ptch1, smo, and gli1) as well as genes associated with the msxb-positive signaling center (msxb, pcna) (36). For these studies, we analyzed gene expression at 5dpa in order to identify transcriptional alterations preceding the regenerative deficits observed between 5–9dpa. Quantitative RT-PCR revealed that BTxB-treated fish exhibited a significant increase in the expression of ptch1 ($p<0.05$) and gli1 ($p<0.05$) (Fig 8). No other significant differences were observed. Interestingly, both gli1 and ptch1 are known gli target genes (37), with ptch1 known to potently repress shh signal transduction through a negative feedback loop (38,39). Thus, these studies suggest that BTxB-induced deficits in regenerative outgrowth may be preceded by gli overactivity and overexpression of ptch1, the latter of which is associated with repressed shh signaling downstream.

DISCUSSION

BTx-induced muscle paralysis has been associated with impaired osteogenesis in diverse conditions of bone formation (e.g., development, growth, and healing), yet the mechanisms of neuromuscular regulation underlying these deficits have yet to be identified. As a first step toward understanding the potential for zebrafish to recapitulate pathways mediating neuromuscular-mediated bone pathologies, in this study we developed a BTx model of muscle paralysis in adult animals, and demonstrated its capacity to impair intramembranous ossification during tail fin regeneration.

Our studies demonstrated the potential for intramuscular administration of BTxB to induce muscle paralysis in adult zebrafish in a manner that was transient, dose-dependent, and focal, mirroring the paralytic phenotype broadly observed in animal and human studies (11,12). For example, the time to paralytic onset and dynamics of locomotor recovery in BTxB fish were temporally consistent with BTxB studies in humans demonstrating onset of paralysis 24~48hrs post injection and a mean recovery time of ~8wks (40). In regard to BTx serotype, the sensitivity of adult zebrafish to BTxB was consistent with the impaired

synaptic transmission observed in zebrafish embryos administered the B serotype at similar dosages (41). In contrast, the observed resistance of zebrafish to BTxA differed from the BTxA sensitivity identified in sunfish (42), and may be attributable to species-dependent mutations in SNAP-25 around the BTxA cleavage site (as in Torpedo fish (41)). It is noteworthy that in animal and human studies, variations in BTx dose, concentration, and carrier volume significantly alter paralytic severity, dynamics of onset and recovery, and BTx diffusion from the injection site. By enabling the targeting of specific neuromuscular circuits and the examination of regenerative mechanisms associated with recovery of synaptic transmission, the BTxB model developed herein may provide a valuable complement to genetic models of systemic and terminal paralysis in zebrafish (43).

During tail fin regeneration, BTx induced multi-faceted deficits on bone regenerative function, reminiscent of the osteoanabolic dysfunction observed in mammalian models of bone development and healing. Our studies suggest the potential for multiple osteogenic processes to be under the influence of neuromuscular regulation, including maintenance of bone outgrowth, bone patterning, late-stage osteoblast differentiation, and secondary bone apposition. In identifying these deficits, we implemented several novel modalities for analyzing mineralizing activity that enabled the identification of subtle skeletal phenotypes. For example, using quantitative fluorochrome analysis, we observed a significant shift toward reduced intensity of labeling in BTxB-treated fish, suggesting decreased appositional activity in newly regenerated bone segments. Interestingly, BTxB-injected fish exhibited substantial phenotypic variation in labeling deficits (i.e., different degrees of intra- and inter-ray heterogeneity), which we speculate may be a consequence of distinct neuronal populations being targeted by slight variations in BTxB injection location. In addition, we utilized Rotopol imaging to quantify bone ray birefringence, a measure of crystalline mineral accumulation during regeneration. This quantity was significantly decreased in the regenerated (but not non-regenerated) tissue of BTxB-injected fish, suggesting that BTxB impaired bone mineral accrual in newly regenerating bone but did not systemically induce demineralization in non-regenerated bone tissue.

Given the remote effects of BTxB administration at the base of the tail on fin regrowth at the distal tip, an intriguing question is the role of fin ray nerves in mediating BTxB-induced regenerative defects. Nerve-dependent appendage regeneration has long been observed in diverse contexts and phyla, including limb regeneration in salamanders (44). In our studies, several of the physiological features of BTxB were focal to specific bone rays (e.g., greater inhibition of regrowth in middle rays and marked differences in calcein labeling in neighboring rays in some animals), suggesting that these deficits were not manifested by systemic factors alone. Further, we found that bone ray transection was sufficient to focally inhibit regeneration in the affected ray, implicating intra- and/or inter-ray nerves in modulating bone ray outgrowth. In salamanders, systemic administration of BTx at paralytic doses does not inhibit limb regeneration to the early bud stage (45), consistent with the lack of effect of BTxB on early fin regeneration (<5dpa) observed in our investigations. Interestingly, this suggests that cholinergic transmission, a process long speculated to be dispensible for appendage regeneration (45), may be required for late-stage regenerative functions associated with osteoblastic differentiation and control of osteoblast activity (such as bone mineralization, patterning, and cessation of growth), but not early-stage functions

associated with precursor cell origination (such as epithelial migration, dedifferentiation, and blastema formation). This distinction may have important implications in the potential to infer regulatory mechanisms identified in our model to broader bone anabolic contexts, as dedifferentiation and blastema formation are processes specific to epimorphic regeneration, whereas osteoblastic differentiation is not.

Drawing parallels between the regenerative deficits identified in BTxB-treated fish and phenotypes attributed to known regenerative signaling pathways may provide important clues into underlying mechanisms regulating this pathophysiology. In the regenerating zebrafish fin, two well-characterized signaling centers have been established: the msxb-positive signaling center at the distal blastema (36) (a regulator of cell proliferation in the proximal blastema), and the shh-positive center at the basal epidermal layer (34) (a regulator of continued bone outgrowth, patterning, and bone cell differentiation). Our studies suggest that regenerative deficits in BTxB-treated fish were preceded by overactivity of the shh transcriptional effector gli, as evidenced by the overexpression of the gli target genes gli1 and ptch1 (the latter of which has potential to repress shh signaling downstream). In this context, BTxB-treated fish closely phenocopied fish administered cyclopamine (a chemical inhibitor of shh signaling) in multiple aspects (34), including impaired bone outgrowth during late (but not early) regeneration, lack of bifurcations in the regenerate, and reductions in the number of bone segments. In mammals, shh is a critical regulator of bone patterning and continued outgrowth in the developing limb bud, and recent studies suggest that it is also expressed during early fracture repair (46). Though bone and nerves have long been known to develop and regenerate in concert (e.g., in the developing limb bud and during bone healing), their potential to crosstalk via established regenerative pathways has not been explored. Intriguingly, our studies suggest a potential regulatory link between BTxB-sensitive nerves, shh signaling, and bone cell differentiation/activity that does not require direct contact with skeletal muscle, an exciting avenue for future investigation that may be ideal for cross-examination in zebrafish and more complex animal model systems.

Several limitations should be considered when interpreting the findings from this study. First, while kinematic analyses suggested that locomotor deficits arising from BTxB injection were focal to the injection site, we are unable to rule out the possibility that BTx migrated/diffused to distant tissue sites. However, the fact that bone ray transection in the absence of BTx inhibited bone ray outgrowth suggests that direct binding of BTx to regenerating cells at the distal fin tip was not an essential etiological factor in our studies. Second, regenerative defects in our study may be attributable to either decreased innervation (e.g., stemming from impaired nerve regeneration) or impaired nerve function (e.g., stemming from cholinergic blockade), and we did not delineate these possibilities. The examination of re-innervation in the regenerate following BTx may provide important insight in this regard, and we are actively pursuing such studies. Finally, given that ray-associated blood vessels were severed in our fin ray transection model, as well as evidence that blood vessels may guide bone ray patterning (47), at this time we are unable to rule out the possibility that impaired vascular function contributed to the observed effects on focal bone ray outgrowth. The use of laser-based axotomies (48) may enable precise delineation of vascular, intra-ray nerve, and inter-ray nerve contributions to bone ray growth, as well as the contribution of specific nerve populations to this process.

In summary, our studies are the first to demonstrate the potential to examine features of BTx-mediated bone anabolic dysfunction in the regenerating zebrafish fin, and suggest that pathways mediating neuromuscular regulation of osteogenesis may be conserved beyond established mammalian models of bone anabolic disorders. Given the experimental flexibility of zebrafish, these studies provide an essential starting point for the development of rapid *in vivo* screening modalities for neuromuscular-mediated bone anabolic pathologies, as well as novel models of neuro-musculoskeletal systems biology that elucidate mechanisms of nerve-muscle-bone crosstalk during their co-development, ontogenesis, and regeneration.

Acknowledgments

Author roles: Designed research: AMR, ACR, RYK. Conducted research: AMR, ACR, MS, LEW, TP, NS, RYK. Analyzed/interpreted data: All authors. Drafted manuscript: RYK. Revised manuscript: All authors. Approved final manuscript: All authors. RYK takes responsibility for the integrity of the data analysis. The authors would like to acknowledge the following financial support: Mary Gates Endowment for Students (AMR), National Institutes of Health (SS: R01 AR056235, TSG: R01 AR056652, NS: T32 GM07270), the Zimmer Fracture Biology Professorship (SDB), the Sigvard T. Hansen, Jr. Endowed Chair (TSG), the UW Department of Orthopaedics and Sports Medicine (ACR: Resident Research Grant, RYK: New Faculty Research Fund and startup support), and the UW Royalty Research Fund (RYK).

References

1. Lieschke GJ, Currie PD. Animal models of human disease: zebrafish swim into view. Nature Reviews Genetics. 2007; 8(5):353–367.
2. Apschner A, Schulte-Merker S, Witten PE. Not all bones are created equal – using zebrafish and other teleost species in osteogenesis research. Methods in Cell Biology. 2011; 105:239–255. [PubMed: 21951533]
3. Renn J, Winkler C, Schartl M, Fischer R, Goerlich R. Zebrafish and medaka as models for bone research including implications regarding space-related issues. Protoplasma. 2006; 229(2–4):209–214. [PubMed: 17180503]
4. Barrett R, Chappell C, Quick M, Fleming A. A rapid, high content, in vivo model of glucocorticoid-induced osteoporosis. Biotechnology Journal. 2006; 1(6):651–655. [PubMed: 16892313]
5. Siccardi AJ III, Padgett-Vasquez S, Garris HW, Nagy TR, D'Abramo LR, Watts SA. Dietary strontium increases bone mineral density in intact zebrafish (Danio rerio): A potential model system for bone research. Zebrafish. 2010; 7(3):267–273. [PubMed: 20874492]
6. Rivadeneira F, et al. Twenty bone-mineral-density loci identified by large-scale meta-analysis of genome-wide association studies. Nature Genetics. 2009; 41(11):1199–1206. [PubMed: 19801982]
7. Spoorendonk KM, Hammond CL, Huitema LFA, Vanoevelen J. Zebrafish as a unique model system in bone research: the power of genetics and in vivo imaging. Journal of Applied Ichthyology. 2010; 26(2):219–224.
8. Andreeva V, Connoly MH, Stewart-Swift C, Fraher D, Burt J, Cardarelli J, Yelick PC. Identification of adult mineralized tissue zebrafish mutants. Genesis. 2011; 49(4):360–366. [PubMed: 21225658]
9. Kwon RY, Meays DR, Tang WJ, Frangos JA. Microfluidic enhancement of intramedullary pressure increases interstitial fluid flow and inhibits bone loss in hindlimb suspended mice. Journal of Bone and Mineral Research. 2010; 25(8):1798–1807. [PubMed: 20200992]
10. Kwon RY, Meays DR, Meilan AS, Jones J, Miramontes R, Kardos N, Yeh JC, Frangos JA. Skeletal adaptation to intramedullary pressure-induced interstitial fluid flow is enhanced in mice subjected to targeted osteocyte ablation. PloS One. 2012; 7(3):e33336. [PubMed: 22413015]
11. Poliachik SL, Bain SD, Threet D, Huber P, Gross TS. Transient muscle paralysis disrupts bone homeostasis by rapid degradation of bone morphology. Bone. 2010; 46(1):18–23. [PubMed: 19857614]

12. Warner SE, Sanford DA, Becker BA, Bain SD, Srinivasan S, Gross TS. Botox induced muscle paralysis rapidly degrades bone. Bone. 2006; 38(2):257–264. [PubMed: 16185943]
13. Warden SJ, Galley MR, Richard JS, George LA, Dirks RC, Guildenbecher EA, Judd AM, Robling AG, Fuchs RK. Reduced gravitational loading does not account for the skeletal effect of botulinum toxin-induced muscle inhibition suggesting a direct effect of muscle on bone. Bone. 2013; 54(1): 98–105. [PubMed: 23388417]
14. Bain SD, Poliachik SL, Threet D, Srinivasan S, Gross TS. Trabecular bone homeostasis is modulated by neuromuscular proprioception. Journal of Bone and Mineral Research. 2010; 25(S1):SU0106.
15. Kim HM, Galatz LM, Patel N, Das R, Thomopoulos S. Recovery potential after postnatal shoulder paralysis. An animal model of neonatal brachial plexus palsy. Journal of Bone and Joint Surgery. 2009; 91(4):879–891. [PubMed: 19339573]
16. Hao Y, Ma Y, Wang X, Jin F, Ge S. Short-term muscle atrophy caused by botulinum toxin-A local injection impairs fracture healing in the rat femur. Journal of Orthopaedic Research. 2011; 30(4): 574–580. [PubMed: 21919046]
17. Rauch F, Hamdy R. Effect of a single botulinum toxin injection on bone development in growing rabbits. Journal of Musculoskeletal & Neuronal Interactions. 2006; 6(3):264–268. [PubMed: 17142948]
18. Bain SD, Prasad J, Wiater B, Huber P, Nork S, Gross TS. Transient muscle paralysis blocks the osteogenic response to skeletal injury. Journal of Bone and Mineral Research. 2009; 24(S1):SU0096.
19. Tsai CY, Shyr YM, Chiu WC, Lee CM. Bone changes in the mandible following botulinum neurotoxin injections. European Journal of Orthodontics. 2011; 33(2):132–138. [PubMed: 20884720]
20. Iovine MK. Conserved mechanisms regulate outgrowth in zebrafish fins. Nature Chemical Biology. 2007; 3(10):613–618. [PubMed: 17876318]
21. Sousa S, Valerio F, Jacinto A. A new zebrafish bone crush injury model. Biology Open. 2012; 1(9): 915–921. [PubMed: 23213486]
22. Knopf F, Hammond C, Chekuru A, Kurth T, Hans S, Weber CW, Mahatma G, Fisher S, Brand M, Schulte-Merker S, Weidinger G. Bone regenerates via dedifferentiation of osteoblasts in the zebrafish fin. Developmental Cell. 2011; 20(5):713–724. [PubMed: 21571227]
23. Tu S, Johnson SL. Fate restriction in the growing and regenerating zebrafish fin. Developmental Cell. 2011; 20(5):725–732. [PubMed: 21571228]
24. Thummel R, Bai S, Sarras MP Jr, Song P, McDermott J, Brewer J, Perry M, Zhang X, Hyde DR, Godwin AR. Inhibition of zebrafish fin regeneration using in vivo electroporation of morpholinos against fgfr1 and msxb. Developmental Dynamics. 2006; 235(2):336–346. [PubMed: 16273523]
25. Johnson SL, Weston JA. Temperature-sensitive mutations that cause stage-specific defects in zebrafish fin regeneration. Genetics. 1996; 141(4):1583–1595.
26. Oppedal D, Goldsmith MI. A chemical screen to identify novel inhibitors of fin regeneration in zebrafish. Zebrafish. 2010; 7(1):53–60. [PubMed: 20384483]
27. Hyde DR, Godwin AR, Thummel R. In vivo electroporation of morpholinos into the regenerating adult zebrafish tail fin. Journal of Visualized Experiments. 2012; 61:3632.
28. Goldshmit Y, Sztal TE, Jusuf PR, Hall TE, Nguyen-Chi M, Currie PD. FGF-dependent glial cell bridges facilitate spinal cord regeneration in zebrafish. The Journal of Neuroscience. 2012; 32(22): 7477–7492. [PubMed: 22649227]
29. Du SJ, Frenkel V, Kindschi G, Zohar Y. Visualizing normal and defective bone development in zebrafish embryos using the fluorescent chromophore calcein. Developmental Biology. 2001; 238(2):239–246. [PubMed: 11784007]
30. Glazer AM, Lewis JG, Kaminsky W. An automatic optical imaging system for birefringent media. Proceedings of the Royal Society of London A. 1996; 452(1955):2751–2765.
31. Worton LE, Ausk BJ, Downey LM, Bain SD, Gardiner EM, Srinivasan S, Gross TS, Kwon RY. Systems-based identification of temporal processing pathways during bone cell mechanotransduction. PLoS One. 2013; 8(9):e74205. [PubMed: 24040202]

32. Kimmel CB, Patterson J, Kimmel RO. The development and behavioral characteristics of the startle response in the zebra fish. Developmental Psychobiology. 1974; 7(1):47–60. [PubMed: 4812270]
33. Stoick-Cooper CL, Weidinger G, Riehle KJ, Hubbert C, Major MB, Fausto N, Moon RT. Distinct Wnt signaling pathways have opposing roles in appendage regeneration. Development. 2007; 134(3):479–489. [PubMed: 17185322]
34. Quint E, Smith A, Avaron F, Laforest L, J M, Gaffield W, Akimenko MA. Bone patterning is altered in the regenerating zebrafish caudal fin after ectopic expression of sonic hedgehog and bmp2b or exposure to cyclopamine. Proceedings of the National Academy of Sciences. 2002; 99(13):8713–8718.
35. Mahamid J, Sharir A, Addadi L, Weiner S. Amorphous calcium phosphate is a major component of the forming fin bones of zebrafish: Indications for an amorphous precursor phase. Proceedings of the National Academy of Sciences. 2008; 105(35):12748–12753.
36. Poss KD, Nechiporuk A, Hillam AM, Johnson SL, Keating MT. Mps1 defines a proximal blastemal proliferative compartment essential for zebrafish fin regeneration. Development. 2002; 129(22):5141–5149. [PubMed: 12399306]
37. Nolan-Stevaux O, Lau J, Truitt ML, Chu GC, Hebrok M, Fernández-Zapico ME, Hanahan D. GLI1 is regulated through Smoothened-independent mechanisms in neoplastic pancreatic ducts and mediates PDAC cell survival and transformation. Genes & Development. 2009; 23(1):24–36. [PubMed: 19136624]
38. Taipale J, Cooper MK, Maiti T, Beachy PA. Patched acts catalytically to suppress the activity of Smoothened. Nature. 2002; 418(6900):892–897. [PubMed: 12192414]
39. Lai K, Robertson MJ, Schaffer DV. The sonic hedgehog signaling system as a bistable genetic switch. Biophysical Journal. 2004; 86(5):2748–2757. [PubMed: 15111393]
40. Sadick NS. Botulinum toxin type B for glabellar wrinkles: a prospective open-label response study. Dermatologic Surgery. 2002; 28(9):817–821. [PubMed: 12269875]
41. Nevin LM, Taylor MR, Baier H. Hardwiring of fine synaptic layers in the zebrafish visual pathway. Neural Development. 2008; 3:36. [PubMed: 19087349]
42. O'Neill MW, Gibb AC. Botulinum toxin injections as a method for chemically denervating skeletal muscle to test funtional hypothesis: a pilot study in Lepomis cyanellus. Physiological and Biochemical Zoology. 2007; 80(2):241–249. [PubMed: 17252520]
43. Granato M, van Eeden FJ, Schach U, Trowe T, Brand M, Furutani-Seiki M, Haffter P, Hammerschmidt M, Heisenberg CP, Jiang YJ, Kane DA, Kelsh RN, Mullins MC, Odenthal J, Nüsslein-Volhard C. Genes controlling and mediating locomotion behavior of the zebrafish embryo and larva. Development. 1996; 123:399–413. [PubMed: 9007258]
44. Kumar A, Brockes JP. Nerve dependence in tissue, organ, and appendage regeneration. Trends in Neurosciences. 2012; 35(11):691–699. [PubMed: 22989534]
45. Drachman DB, Singer M. Regeneration in botulinum-posioned forelimbs of the newt, Triturus. Experimental Neurology. 1971; 31(1):1–11. [PubMed: 4101944]
46. Miyaji T, Nakase T, Iwasaki M, Kuriyama K, Tamai N, Higuchi C, Myoui A, Tomita T, Yoshikawa H. Expression and distribution of transcripts for sonic hedgehog in the early phase of fracture repair. Histochemistry and Cell Biology. 2003; 119(3):233–237. [PubMed: 12649738]
47. Huang CC, Wang TC, Lin BH, Wang YW, Johnson SL, Yu J. Collagen IX is required for the integrity of collagen II fibrils and the regulation of vascular plexus formation in zebrafish caudal fins. Developmental Biology. 2009; 332(2):360–370. [PubMed: 19501583]
48. Rosenberg AF, Wolman MA, Franzini-Armstrong C, Granato M. In vivo nerve-macrophage interactions following peripheral nerve injury. Journal of Neuroscience. 2012; 32(11):3898–3909. [PubMed: 22423110]

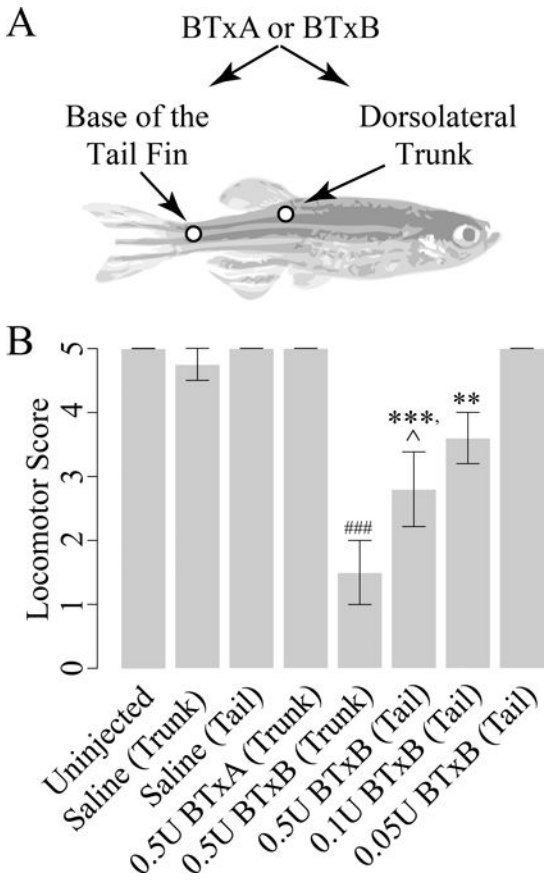

Figure 1. Intramuscular administration of BTxB, but not BTxA, inhibits locomotor function in zebrafish in a dose- and site-specific manner

(A) Schematic depicting injection locations. (B) Locomotor scores at 3dpi. **: $p<0.01$, ***: $p<0.001$ vs. tail-injected fish administered saline; ###: $p<0.001$ vs. trunk-injected fish administered saline; ^: $p<0.05$ vs. trunk-injected fish administered equivalent dose of BTxB; n=2–5/group.

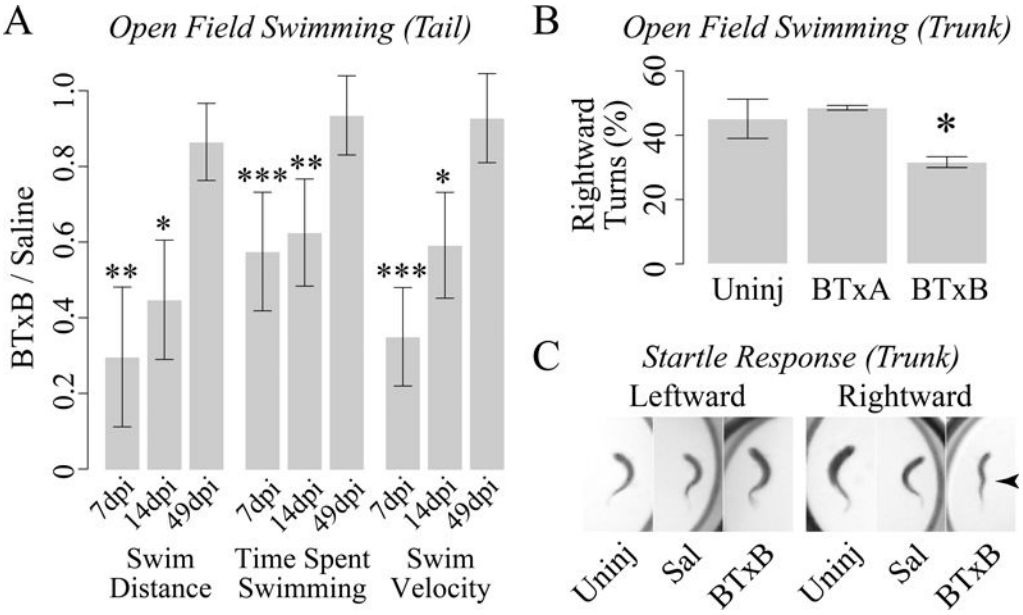

Figure 2. BTxB-induced paralysis is transient and focal

(A) Tail-injected fish administered BTxB exhibit impaired open field swimming activity at 7dpi (days post injection) and 14dpi but not 49dpi. *: $p<0.05$, **: $p<0.01$, ***: $p<0.001$ for BTxB vs. saline; n>6/group. (B) Trunk-injected fish administered BTxB exhibit a decrease in the number of rightward (clockwise) turns during open field swimming. *: $p<0.05$ for difference in proportions between leftward and rightward turns; n=2–3/group. (C) Trunk-injected fish administered BTxB (but not saline-injected fish or uninjected controls) exhibit a kinked-shaped body plan (arrow) during rightward (clockwise), but not leftward (counter-clockwise) turns.

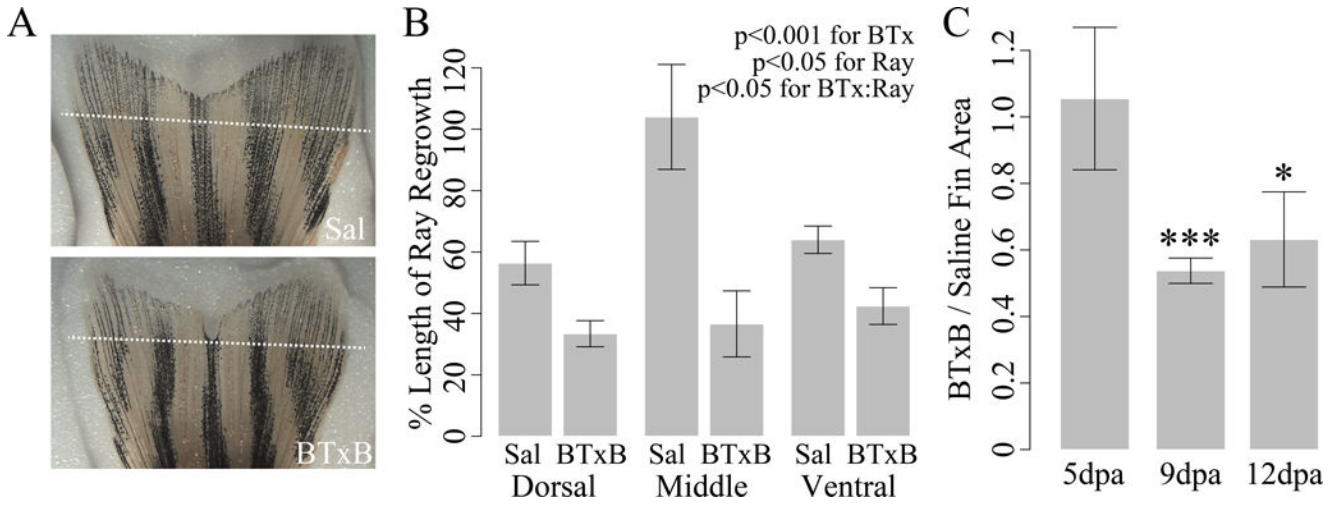

Figure 3. BTxB impairs bone ray outgrowth in a site- and time-dependent manner during fin regeneration

(A) Brightfield images of tail fins (9dpa) in saline- and BTxB-injected fish. (B) Quantification of percent length regrowth (9dpa). Relative difference between BTxB and saline-injected fish is greatest in the middle bone rays. n=5/group. (C) Relative difference in regenerated fin area at 5dpa, 9dpa, and 12dpa. *: $p<0.05$, ***: $p<0.001$ for BTxB vs. saline; n=5–8/group.

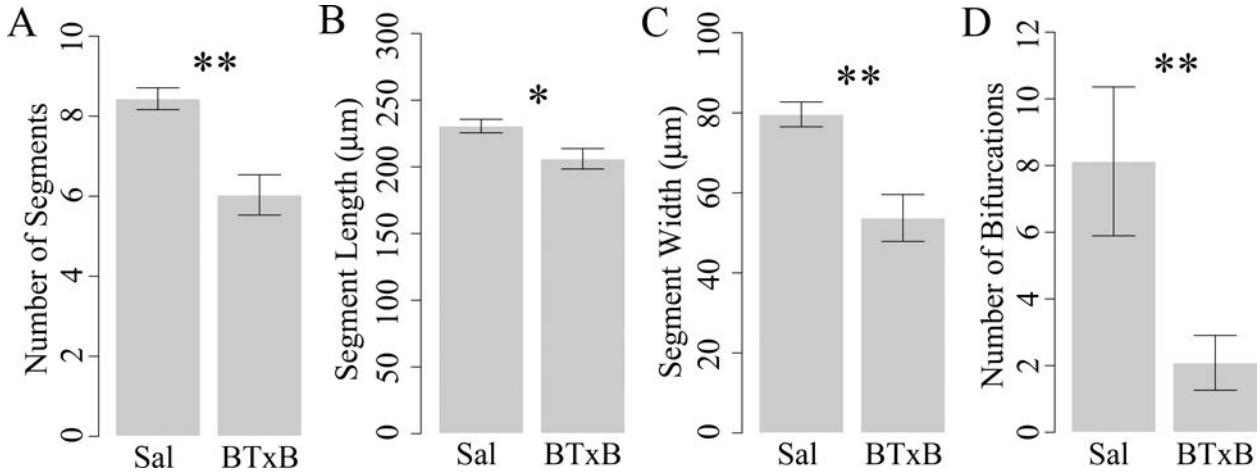

Figure 4. BTxB alters bone ray segment morphology, joint specification, and patterning during fin regeneration at 9dpa

Results shown for (A) number of segments, (B) segment length (i.e., inter-joint distance), (C) segment width, and (D) number of bifurcations. *: $p<0.05$, **: $p<0.01$ for BTxB vs. saline; n=5/group.

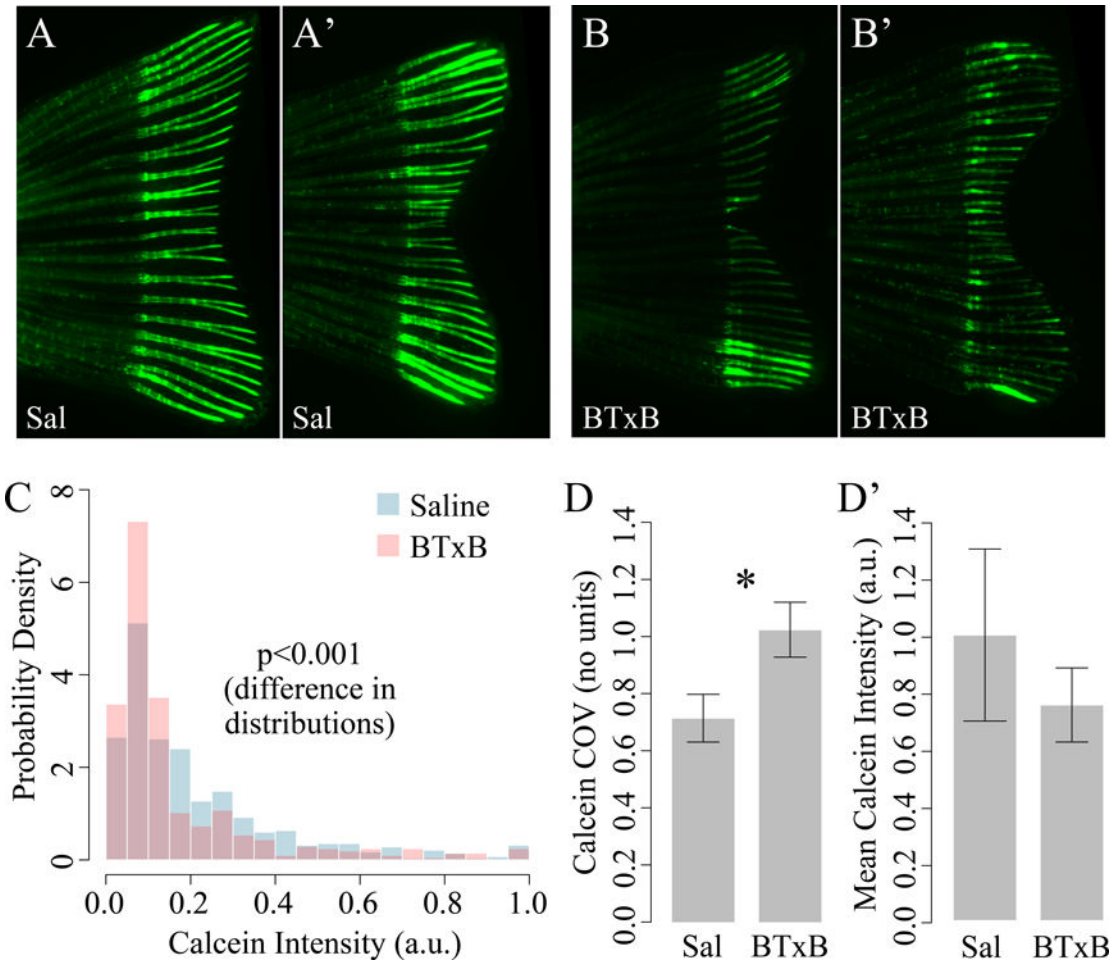

Figure 5. BTxB-injected fish exhibit altered calcein labeling characterized by increased intra- and inter-ray heterogeneity and an overall shift toward lower intensity

(A–A′) Fluorescent images of calcein labeling in two saline-injected fish (9dpa). (B–B′) Fluorescent images of calcein labeling in two BTxB-injected fish (9dpa). Note the marked differences in labeling between neighboring rays in (B) and within rays in (B′). (C) Probability distributions for calcein intensity in saline- and BTxB-injected fish. (D) Coefficient of variation (a measure of dispersion) for calcein intensity is significantly increased in BTxB-treated fish. (E) No significant difference in mean intensity is observed. *: $p<0.05$, for BTxB vs. saline; n=5/group.

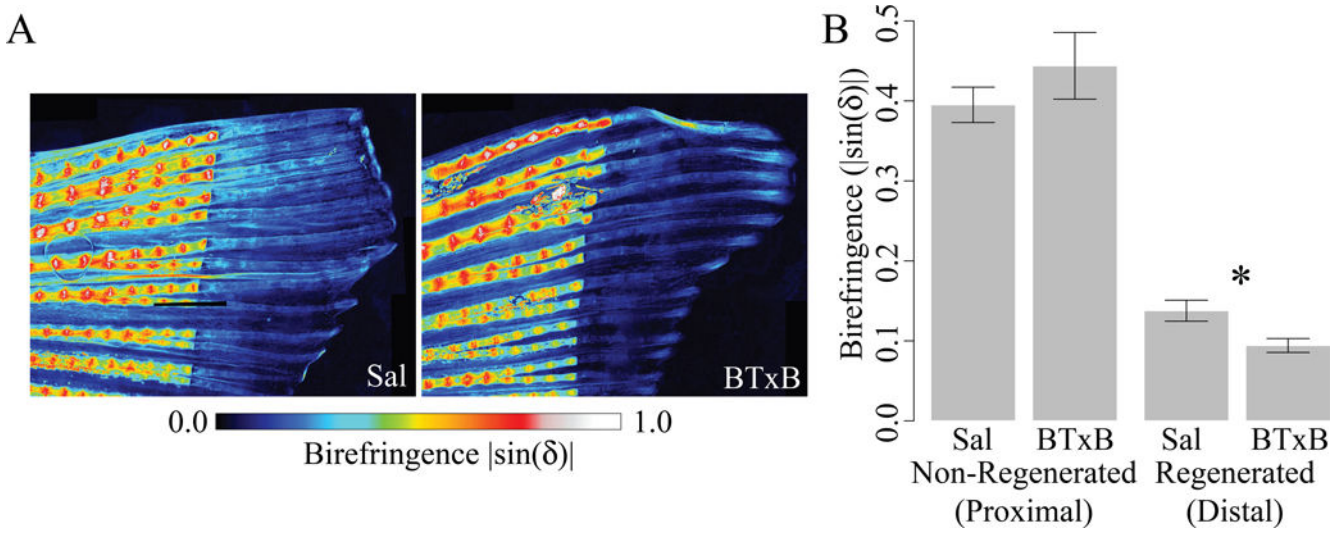

Figure 6. BTxB-treated fish exhibit decreased crystalline mineral accumulation in regenerated (distal to the amputation plane), but not non-regenerated (proximal to the amputation plane) tissue

(A) Rotopol images of birefringence in the ventral fin of saline- and BTxB-injected fish (9dpa). (B) Birefringence in non-regenerated and regenerated tissue. *: $p<0.05$ for BTxB vs. saline; n=4–5/group.

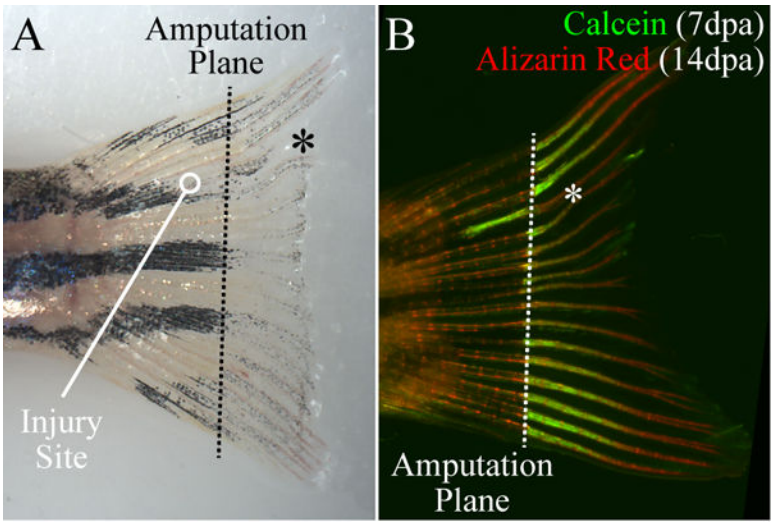

Figure 7. Bone ray transection proximal to the amputation site focally inhibits bone outgrowth

(A) Fin regrowth at 7dpa. Bone growth in the damaged ray (*) is visibly shorter than in the neighboring rays. (B) Double fluorochrome labeling 7dpa (calcein) and 14dpa (alizarin red). Calcein labeling is markedly reduced in the regenerated portion of the damaged ray (*). Note also the increased calcein labeling at the site of injury.

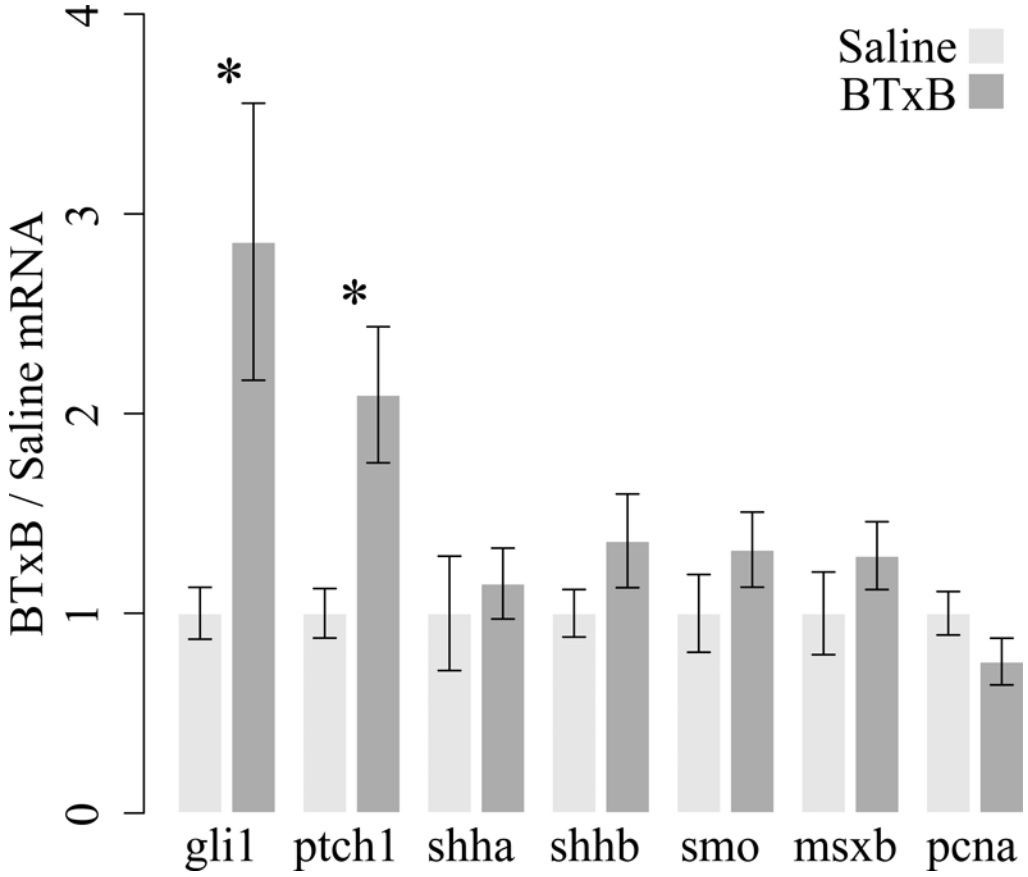

Figure 8. BTxB alters sonic hedgehog pathway gene expression

Gene expression was assessed at 5dpa via real time RT-PCR. Results are shown for genes associated with the sonic hedgehog pathway (shha, shhb, smo, ptch1, gli1) and the msxb-positive signaling center (msxb and pcna). *: $p<0.05$ for BTxB vs. saline; n=4–6/group.